Supporting Information

Overcoming Pd/TiO_2 Deactivation during H_2 Production from Photoreforming by Using Cu@Pd Nanoparticles Supported on TiO_2

*F. Platero[a], A. López-Martín[a], A. Caballero[a], T.C. Rojas[a], M. Nolan[b], G. Colón[a] **

[a] Instituto de Ciencia de Materiales de Sevilla. Centro Mixto Universidad de Sevilla-CSIC. Américo Vespucio s/n. 41092 Sevilla. Spain

[b] Tyndall National Institute, University College Cork, Lee Maltings, Dyke Parade, Cork, T12 R5CP Ireland

* Corresponding author: gcolon@icmse.csic.es

Table S1. Intermediate evolution in the liquid phase during isopropanol photoreforming reaction (max. indicates the time at which higher signal is observed).

	1 hour	2 hours	3 hours	4 hours	5 hours
$Pd_{1.0}$		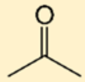		 (max)	
		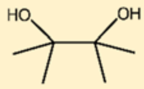	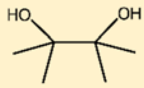	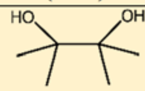 (max)	
$Cu_{2.0}$	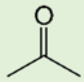	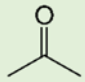	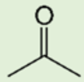	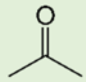	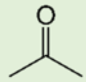 (max)
					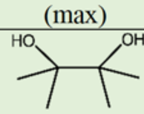 (max)
$Pd_{1.0}Cu$	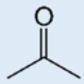	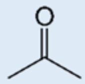	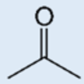	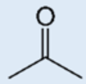	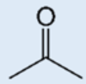 (max)
					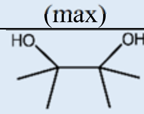 (max)

Acetone	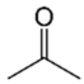
Pinacol: 2,3-dimethyl-2,3-butanediol	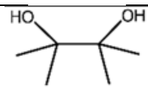

Table S2. Apparent quantum efficiencies (AQE) calculated from reaction rates at 5 and 18 hours for monometallic Cu,Pd and bimetallic Cu@Pd/TiO_2 systems.

Pd (mol%)	AQE after 5 hours		AQE after 18 hours	
	Pd/TiO_2	Cu@Pd/TiO_2	Pd/TiO_2	Cu@Pd/TiO_2
0	---	4.14	--	2.95
0.03	1.40	4.19	1.35	3.42
0.05	2.59	4.40	2.07	3.88
0.1	5.07	6.05	4.14	4.81
0.2	6.99	7.09	4.14	5.28
0.3	7.76	7.35	4.92	5.69
0.4	8.54	7.50	4.40	5.64
0.5	8.02	10.87	4.50	7.71
1.0	7.87	10.40	4.00	7.35

Table S3. Surface and bulk chemical composition of Cu and Pd doped TiO_2 systems.

Samples	ICP-OES			XPS		
	Cu (at %)	Pd (at %)	Pd/Cu	Cu/Ti	Pd/Ti	Pd/Cu
$Pd_{1.0}/TiO_2$	---	1.03	---	---	$14·10^{-3}$	---
$Cu@Pd_{1.0}/TiO_2$	0.30	1.03	2.32	0.01	$18·10^{-3}$	1.79
$Cu@Pd_{0.5}/TiO_2$	0.44	0.55	1.96	0.02	$13·10^{-3}$	0.72
$Cu@Pd_{0.4}/TiO_2$	0.84	0.36	0.42	0.05	$10·10^{-3}$	0.21
$Cu@Pd_{0.3}/TiO_2$	1.38	0.25	0.18	0.08	$9·10^{-3}$	0.09
$Cu@Pd_{0.2}/TiO_2$	2.00	0.15	0.07	0.12	$8·10^{-3}$	0.07
$Cu@Pd_{0.1}/TiO_2$	2.10	0.08	0.02	0.13	$2·10^{-3}$	0.02
$Cu@Pd_{0.05}/TiO_2$	n.d.	n.d.	n.d.	0.13	$1·10^{-3}$	0.01
$Cu_{2.0}/TiO_2$	2.13	---	---	0.13	---	---

Table S4. Structural and surface features of Cu and Pd doped TiO_2 systems.

	BET (m^2/g)	Crystallite size* (nm)	Band-gap (eV)
TiO_2	50	23	3.2
$Pd_{1.0}/TiO_2$	51	25	3.2
$Cu@Pd_{0.3}/TiO_2$	50	22	3.2
$Cu_{2.0}/TiO_2$	51	23	3.2

* Calculated by Rietveld analysis.

Table S5. XPS analysis for Cu and Pd doped TiO_2 systems.

	Cu *2p*$_{3/2}$		Pd *3d*$_{5/2}$	
	BE (EV)	Cu^0/Cu^+ *	BE (eV)	$Pd^0/(Pd^{2+}+Pd^{4+})$**
$Pd_{1.0}/TiO_2$	---	---	334.6	2.8
$Cu@Pd_{1.0}/TiO_2$	931.8	---	334.3	3.3
$Cu@Pd_{0.5}/TiO_2$	931.5	3.50	334.5	1.9
$Cu@Pd_{0.4}/TiO_2$	932.3	0.80	334.5	1.4
$Cu@Pd_{0.3}/TiO_2$	932.4	1.55	334.9	1.5
$Cu@Pd_{0.2}/TiO_2$	932.4	1.82	335.5	1.4
$Cu@Pd_{0.1}/TiO_2$	932.4	1.55	335.5	1.5
$Cu@Pd_{0.05}/TiO_2$	932.4	1.20	334.5	n.d.
$Cu_{2.0}/TiO_2$	932.4	0.94	1.92	---

* Cu^0/Cu^+ ratio calculated from the Cu *LMM* relative intensities for Cu^0 and Cu^+.

** $Pd^0/(Pd^{2+}+Pd^{4+})$ ratio calculated from the deconvolution of Pd *3d* peak.

Table S6: Computed Bader charges (in electrons) for interface Cu atoms, surface Cu/Pd atoms and reduced Ti atoms in the TiO_2 support. The net charge is the difference between the computed charge and the number of valance electrons. The number of valance electrons is 11 for Cu, 4 for Ti, 16 for Pd and 6 for oxygen.

Structure			
Cu/TiO_2	**Cu@Pd_1-TiO_2**	**Cu-core-Pd-shell-TiO_2**	**Pd/TiO_2**
Interface Cu	*Interface Cu*	*Interface Cu*	*Interface Pd*
10.74 – 10.81	10.73-10.8	10.70-10.79	15.78 – 16.08
Surface Cu	*Surface Cu/ Surface Pd*	*Surface Pd*	*Surface Pd*
10.98 – 11.0	10.85 – 10.90 (Cu) 16.28 (Pd)	10.74 – 10.90 (Cu) 16.05 – 16.1 (Pd)	16
Ti in TiO_2	*Ti in TiO_2*	*Ti in TiO_2*	*Ti in TiO_2*
1.66, 1.72, 1.72	1.66, 1.72, 1.72	1.66, 1.72, 1.72	1.39, 1.42

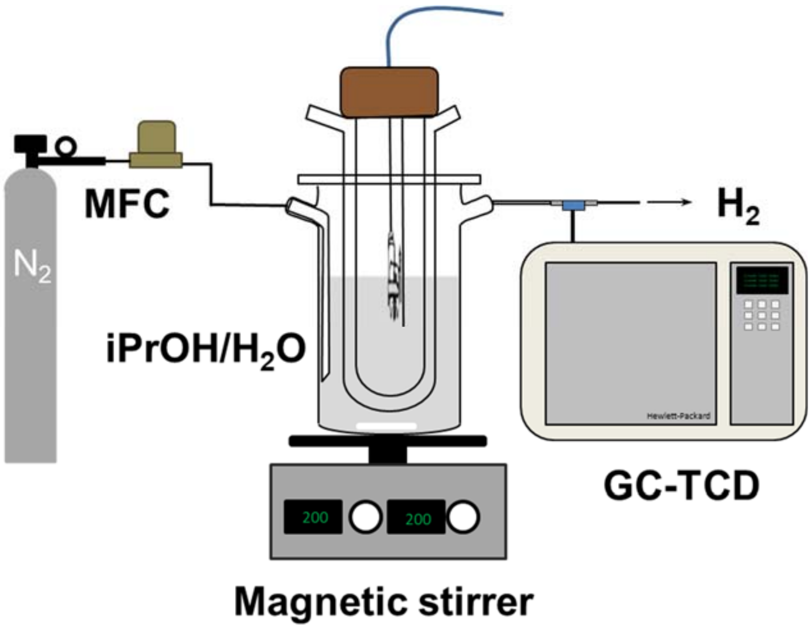

Figure S1. Photocatalytic flow-reactor used for hydrogen production reaction.

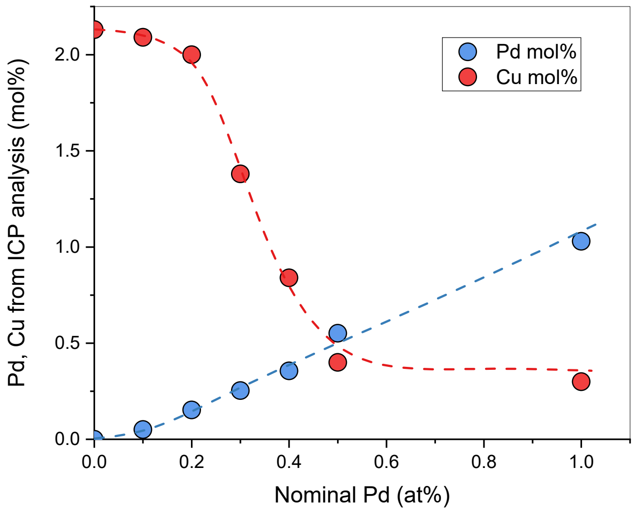

Figure S2. Evolution of Cu and Pd loading measured from ICP analysis with respect to nominal Pd values.

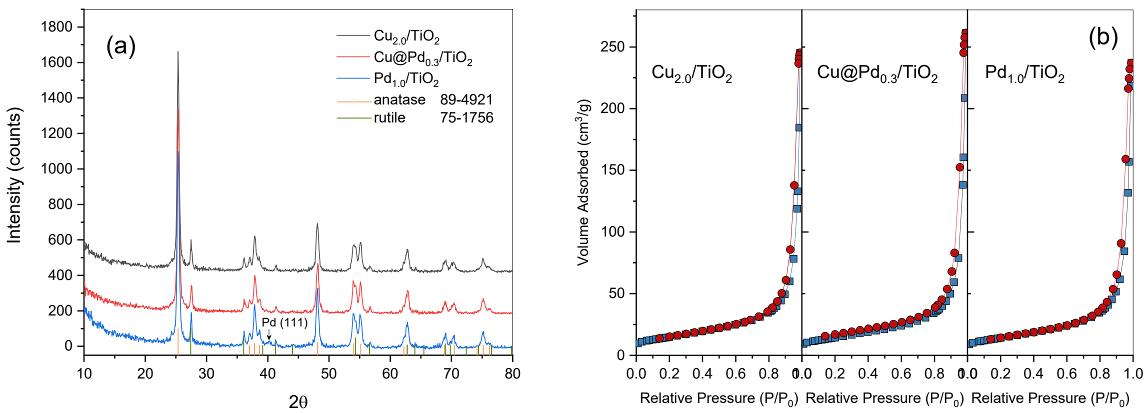

Figure S3. a) XRD pattern and b) N_2 adsorption-desorption isotherms for monometallic Cu/, Pd/ and Cu@$Pd_{0.3}$/TiO_2 systems.

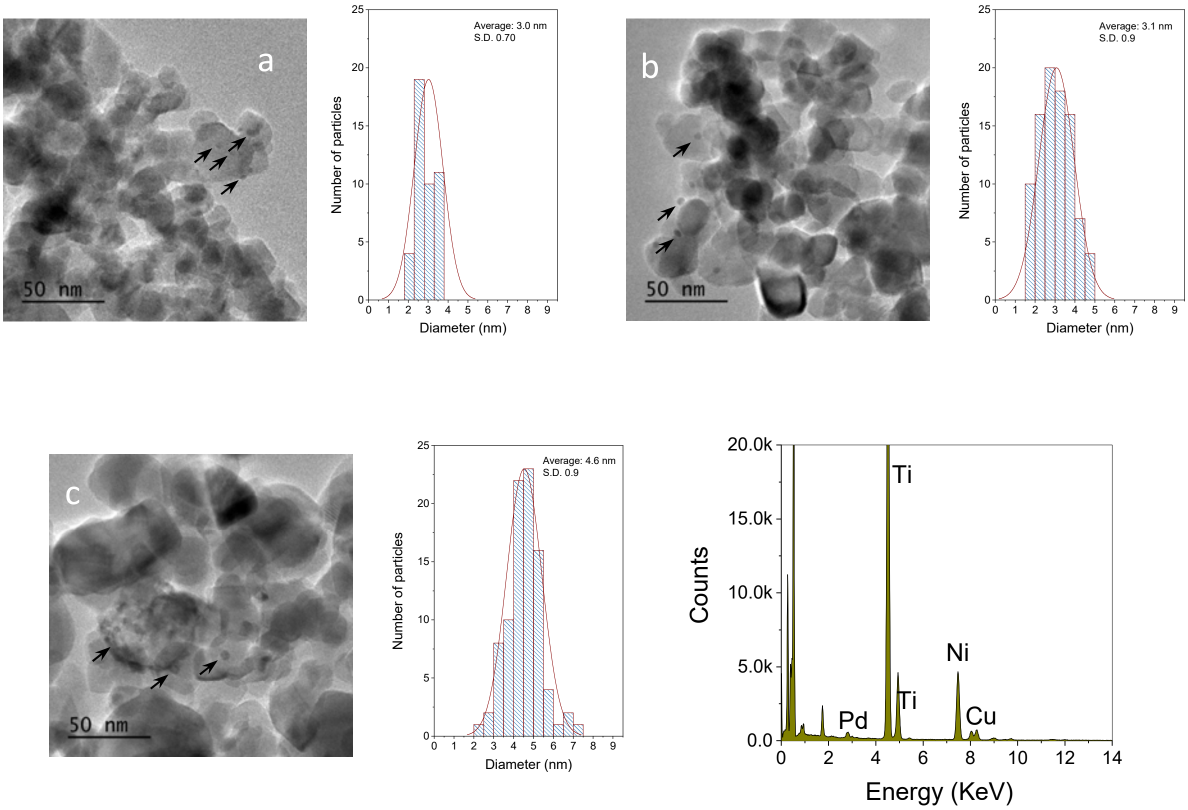

Figure S4. TEM analysis for: a) $Cu@Pd_{0.1}/TiO_2$; b) $Cu@Pd_{0.2}/TiO_2$; and c) $Cu@Pd_{0.3}/TiO_2$ samples.

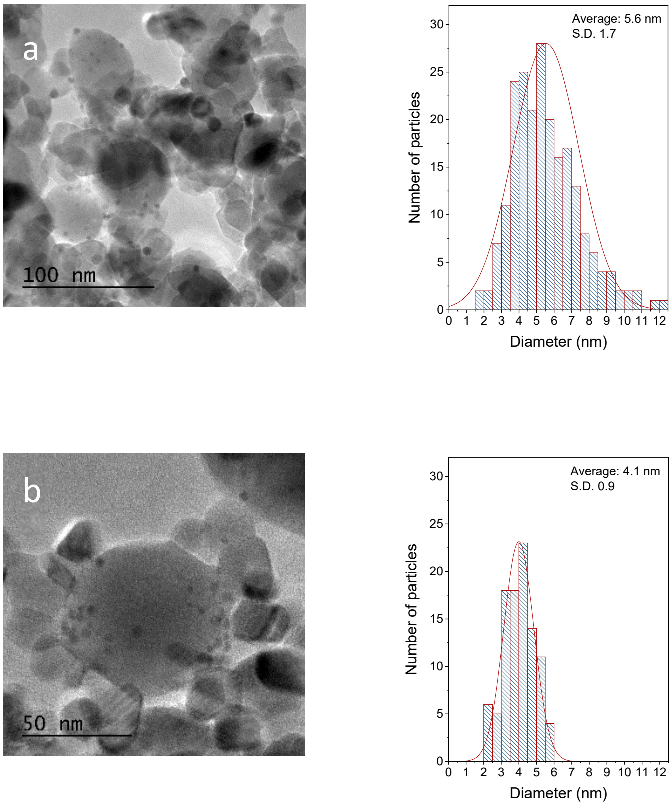

Figure S5. TEM analysis for: a) $Pd_{1.0}/TiO_2$; and b) $Cu@Pd_{1.0}/TiO_2$ samples after 5 hours of reaction.

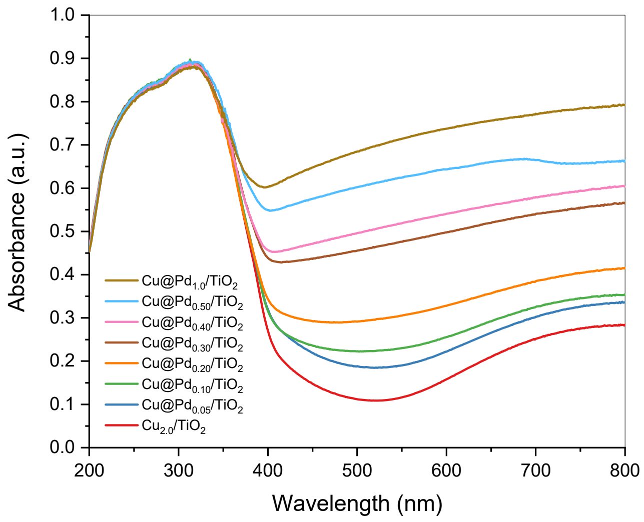

Figure S6. Diffuse reflectance UV-vis spectra for Cu@Pd/TiO_2 systems.

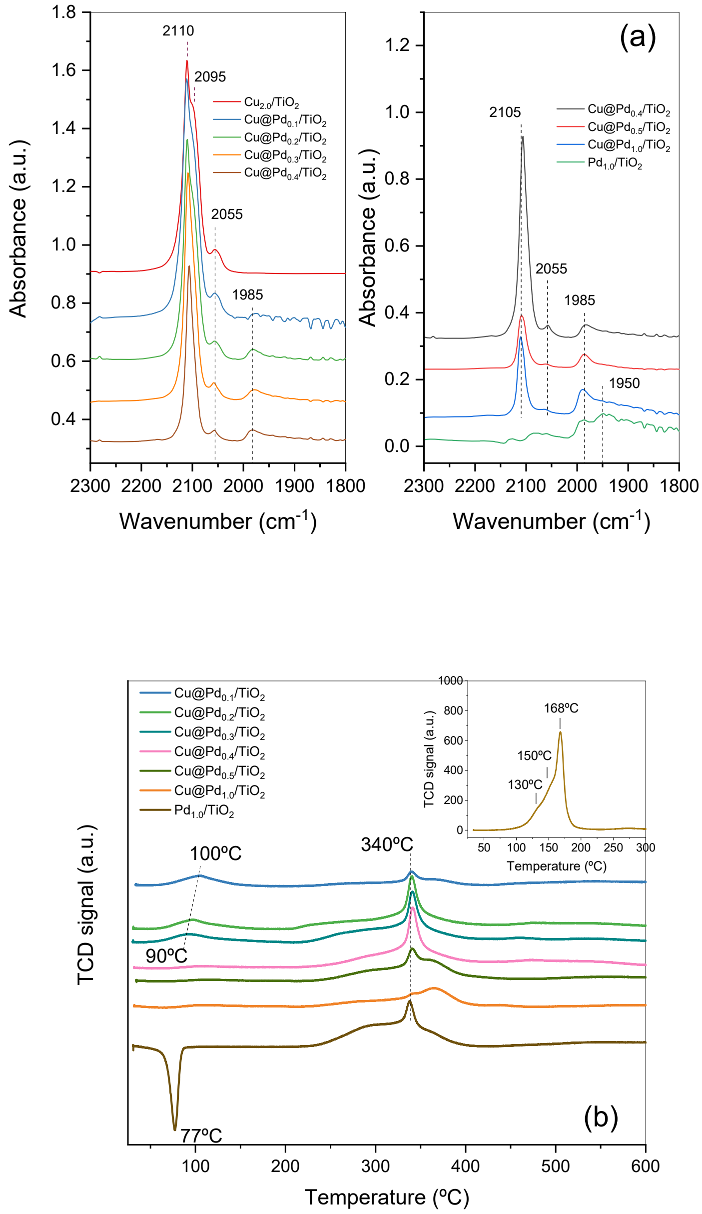

Figure S7. a) FTIR spectra of CO irreversibly adsorbed; b) H_2-TPR curves for different Cu@Pd doped TiO_2 systems. Inset: H_2-TPR for $Cu_{2.0}/TiO_2$.